Research Square

Preprints are preliminary reports that have not undergone peer review.
They should not be considered conclusive, used to inform clinical practice,
or referenced by the media as validated information.

In-Process measurement of tool displacement in ultrasonic vibration superimposed turning of bronze

Jonas Maximilian Werner

jonas-maximilian.werner@mb.tu-chemnitz.de

TU Chemnitz: Technische Universitat Chemnitz https://orcid.org/0009-0002-9163-1600

Hendrik Liborius

TU Chemnitz: Technische Universitat Chemnitz

Andreas Schubert

TU Chemnitz: Technische Universitat Chemnitz

Welf-Guntram Drossel

TU Chemnitz: Technische Universitat Chemnitz

Research Article

Keywords: Ultrasonic-assisted machining, in-process-monitoring, microstructuring, vibration-superimposed turning

Posted Date: November 10th, 2026

DOI: https://doi.org/10.21203/rs.3.rs-11350282/v1

License: This work is licensed under a Creative Commons Attribution 4.0 International License.
Read Full License

In-Process measurement of tool displacement in ultrasonic vibration superimposed turning of bronze

Jonas Maximilian Werner[1*], Hendrik Liborius[2], Andreas Schubert[2], Welf-Guntram Drossel[1,3]

[1*]Professorship Adaptronics and Lightweight Design, TU Chemnitz, Reichenhainer Straße 70, Chemnitz, 09126, Saxony, Germany.
[2]Professorship Micromanufacturing Technology, TU Chemnitz, Reichenhainer Straße 70, Chemnitz, 09126, Saxony, Germany.
[3]Fraunhofer Institute for Machine tools and Forming Technology, Reichenhainer Straße 88, Chemnitz, 09126, Saxony, Germany.

*Corresponding author(s). E-mail(s): jonas-maximilian.werner@mb.tu-chemnitz.de;

Abstract

Ultrasonic vibration-superimposed turning can be used to improve the performance of components by enabling a surface microstructuring in finish machining. Even though the benefits are numerous, control of the vibration amplitude and operating frequency during machining proves difficult as mechanical and electrical resonance frequencies do not always match, limiting their efficiency and use in industrial applications. This highlights the need for improvement of conventional control systems. Measuring mechanical vibrations close to the cutting tool might offer benefits regarding the precision of displacement control compared to conventional approaches like phase-locked loop. To examine the usability and the information content of physical measurands, a sonotrode is designed to enable the measurement of acceleration, strain and temperature during machining. For this an accelerometer, fiber-optical sensors and a passive piezoelectric disk in the ultrasonic transducer are considered. Experiments during free vibration and in an ultrasonic vibration-superimposed turning process were carried out and compared to numerical results. Turning experiments were conducted at feeds of 0.05 mm and 0.10 mm and cutting speeds of 120 m/min and 480 m/min. Additionally, power levels of the ultrasonic system and tool flank wear land width were varied. Also, possible sources of deviations between the manufactured and predicted surface were analyzed. The results demonstrate correlations between the sensor data and the surface topography. Thus, the sensors provide meaningful information regarding the dynamic behavior of the system during operation, enabling a process monitoring close to the tool and showing a possible use for a future control system.

Keywords: Ultrasonic-assisted machining, in-process-monitoring, microstructuring, vibration-superimposed turning

1 Introduction

Hybrid manufacturing processes are an approach to overcome the limitations of conventional machining processes. Ultrasonic vibration-assisted processes come with a tremendous number of benefits, when properly configured. In forming processes applying vibrations can

reduce forming forces and increase formability [1, 2]. Ultrasonic welding is used to join plastics, metals or even ceramic materials [3]. In machining processes lower process forces, better chip breakage, less burr, longer tool life, specific build-up of compressive stresses in the material and the machining of hard-to-machine materials like ceramics have been documented [4–9]. Also a combination of vibrations in two or more directions can be used to further enhance the machining process [10], e.g. for elliptical cutting of tungsten [11]. To achieve these advantages the process needs to be designed carefully as factors of the ultrasonic system, e.g. operating frequency, vibration amplitude at the tool and the direction of the vibration affect the outcome substantially. The mechanisms behind these effects have been studied intensively in the literature [12]. The setup for ultrasonic-assisted machining processes usually consists of an ultrasonic signal generator, an optional amplifier, an ultrasonic transducer converting the electrical into a mechanical vibration (mostly using a piezoelectric stack actuator) as well as an application specific sonotrode [13, 14]. The generator supplies a voltage driving the transducer at its resonance frequency to achieve the highest effiency. The sonotrode needs to be designed for each specific application individually and can therefore come in a variety of shapes [15–18]. For cutting processes the tool is usually placed at the front end of the sonotrode where the vibration amplitude is highest.

One application of ultrasonic-assisted machining is the microstructuring of surfaces in a finish turning process [19–23]. Other applications of applying ultrasonic vibrations in a finishing process have been carried out to improve the machining performance of hardened steel [24]. Forces from the cutting process and thermal influences cause a changing load on the ultrasonic system. Therefore the dynamic properties are affected, which may cause a shift of the resonance frequency during operation. To ensure a consistent and reproducible distribution of the microstructures on the surface, control of the operating frequency and vibration amplitude under changing loads is essential. Control systems for ultrasonic systems are usually based on the electrical feedback from the transducer, e.g. current, voltage, power or the phase shift between voltage and current. Common control systems like phase-locked-loop or autoresonant control try to keep the operating frequency close to the current resonance frequency of the system [25]. The main benefit of using the electrical feedback is that the signals themselves are readily available from the transducer and enable a good fit of the resonance frequency during operation. However, as the gathered data is physically far away from the cutting edge [26] information close to the tool might offer better information regarding the mechanical vibration and the displacement at the tool during operation. Mechanical measurands, e.g. displacement, acceleration or strain might enable a more precise monitoring and control of the system behavior during operation. In several works this approach has been investigated [27–31]. However, the set of suitable and available sensor solutions for this is limited. Available options are restricted by the machining process as the necessary optical accessibility or the permament fixation in an industrial setting can not be guaranteed. Additionally, restrictions from the ultrasonic vibrations, e.g. necessary sampling rates of the sensors, their cable routing, their dimensions and mass if applied directly to the ultrasonic system heavily limit the available options further. Previous works considered the use of accelerometers [27], strain gauges, structurally integrated piezoceramics and fiber-optical sensors for the monitoring of an ultrasonic system during free vibration and during machining. Strain gauges showed potential, but pose challenges regarding a durable, long-term fixing under the dynamic loads. By distributing several strain gauges along the length and circumference, the static process forces as well as a bending of the sonotrode were identified during operation. However, the bonding of the strain gauges as well as the electrical connections were damaged during operation [32, 33]. Structurally integrated piezoceramics enabled a detection of different vibration shapes of the system under operation, but their use was only evaluated during free vibration in a feasibility study. Also permanent fixation proved difficult as several joints were damaged during operation [34]. Fiber-optical sensors have been tested along with an accelerometer and a passive piezoelectric disk, but have not been examined for an in-process use yet as the cable routing

of the optical fiber proces difficult in a machining process while avoiding a signal loss [33]. The aim of this work is to evaluate the suitability of different sensor solutions for the in-process monitoring of an ultrasonic system during a turning process. The performance of an accelerometer, fiber-optical sensors and a passive piezoelectric disk are analyzed. Also, a numerical model is build to predict the behavior of the ultrasonic system and to compare the gathered data to the model behavior. Additionally, the surface of the machined samples will be analyzed to compare the in-situ information of the vibration to the ex-situ data of the generated microstructure measured with a microscope. The goal is to prove that sensors measuring the mechanical vibration close to the cutting edge can be used to precisely predict the generated microstructure as well as to provide information regarding the change of the resonance frequency during operation and the current vibration amplitude at the tool.

2 Methods

2.1 Design of the ultrasonic system

A research-specific system was designed to enable the implementation in a turning process for the generation of microstructures as well as to enable the application of the sensor systems as described in the following. The transducer consists of three piezoelectric disks made of SONOX P8 (CeramTec GmbH, Plochingen, Germany) with a diameter of 38 mm. Two are working as the actuator, while one is used as a sensor disk. Copper electrodes are used to connect them electrically. Ti6Al4V is used as the material for the front and back masses of the transducer. The preloading of the piezoelectric stack is done with a screw, which is insulated with a PTFE insert. The sonotrode is made of Ti6Al4V. To amplify the displacement generated by the transducer the sonotrode has an exponential tapering to a final diameter of 19 mm. At the node a mount was manufactured where the sonotrode can be clamped during operation. The design of the transducer and sonotrode was done in an iterative approach (design, simulation, experimental analysis) as described sufficiently in various publications [14]. The final sensor concept is shown in Fig. 1. An ultrasonic power generator (ATHENA Technologieberatung GmbH) is used to drive the system during operation.

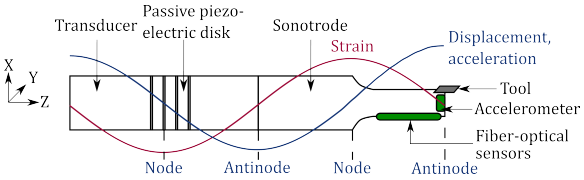


Fig. 1 Distribution of mechanical quantities along the length of an ultrasonic system and proposed sensor concept for the ultrasonic system.

For the numerical analysis a coupled field harmonic analysis was built to analyze the achievable displacements and strains occuring for different operating frequencies to be able to compare them later on with the experimental results. The piezoelectric components were characterized to display structural as well as electrical behaviour. All other components only display structural behavior. Material data was gathered from the manufacturer [35] or experimentally for Ti6Al4V (ρ = 4,420 kg/m^3, E = 108 GPa). For the analysis a frequency range from 20,000 Hz to 26,000 Hz was chosen to identify neighboring resonance frequencies beside the longitudinal vibration. As the harmonic load an electrical voltage up to 100 V was applied to the active piezoceramic disks. The global damping coefficient of 0.0036 is based on experiments of the ultrasonic system. Experiments during free vibration were used to update the material data and the damping coefficient to achieve a good fit between the model and the experiments. The frequency response function of the displacement at the tip of the sonotrode for the longitudinal and transverse vibration is shown in Fig. 2. Additionally, the occuring strain was analyzed and is given in Fig. 4.

2.2 Measuring mechanical vibrations

Mechanical quantities such as strain and displacement have a characteristic distribution along the length of ultrasonic systems as shown in Fig. 1. During vibration a standing wave occurs in the system and the system contracts and expands, inducing areas of high stress and strain with zero displacement, the nodes, and areas of high

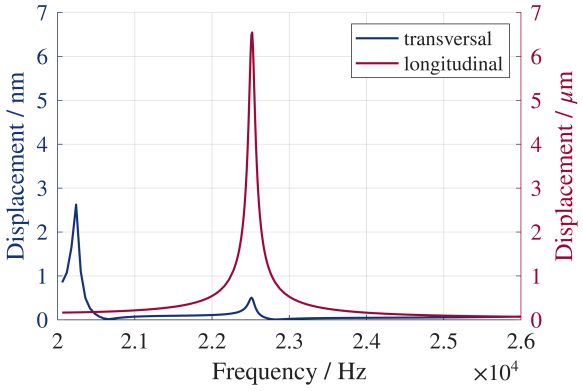


Fig. 2 Frequency response of the longitudinal and transversal vibration at the tip of the sonotrode for $u = 100$ V during free vibration

displacement and zero stress and strain, the antinodes. Ultrasonic systems are mounted at the nodes so as not to dampen the occurring vibration. The tool for the turning process is placed at the antinode to achieve the highest possible displacements.

This behavior has to be considered when choosing suitable sensors as it affects the available sensor positions for different quantities. Additionally requirements from the vibration at an ultrasonic frequency and the machining process have to be considered. For ultrasonic-assisted turning the displacement used is mostly in the range of 10 μm, which corresponds to maximum velocities of 1.58 m/s and maximum accelerations of 250,000 m/s^2 at an operating frequency of 25,000 Hz [36–38]. Additionally, occurring strains did not exceed 400 μm/m in previous works. During operation a build-up of heat might occur caused by dielectric losses in the transducer or caused by the cutting process itself. Therefore, a maximum temperature of 80 °C is set as a limit. Based on this the following sensors were chosen:

- accelerometer (PCB 352A92)
- passive piezoelectric disk (SONOX P8)
- fiber-optical strain and temperature sensor (SM 9/125μ-PI)

To get a better understanding of the relation between the electrical and mechanical vibrations an additional passive piezoelectric disk was added to the transducer. It uses the direct piezoelectric effect. As a material SONOX P8 (Ceramtec GmbH) was chosen. An integration of an additional piezoelectric disk was easily realizable during the design process of the transducer. For measuring the accelerations the accelerometer PCB 352A92 (PCB Synotech GmbH, Hückelhoven, Germany) was chosen. By calculating a double integration of the acceleration data the displacement at the measuring point can be calculated during the process. As shown in Fig. 1 to get the highest signal-noise-ratio the accelerometer should be placed at an antinode close to the cutting tool. The accelerometer was chosen carefully taking a possible cable routing, its mounting on the system, its limitations regarding maximum frequencies and sampling rates and its effects on the dynamic behavior of the ultrasonic system into account. A pocket close to the tool was produced by milling to ensure a safe positioning of the sensor. It was placed along the longitudinal axis of the sonotrode to minimize the risk of an occurring bending mode caused by an uneven weight distribution. As the sensor element only weighs 0.16 g the influence on the dynamic behavior of the system is minimal. The sensor was mounted on the sonotrode using an adhesive.

For measuring the strain several sensor solutions are feasible. Conventional strain gauges have already been used [32]. During preliminary experiments the same approach using strain gauges of the type 10/350 CLY47-3L-2M (HBM/HBK) was chosen, but did not prove to be an expedient solution as the soldering joints as well as the strain gauges themselves were damaged during vibration and were therefore not considered further. As an alternative strain measurement fiber-optical sensors using fiber bragg gratings (FBG) were considered. They have the same benefits of having low weight, also allowing the measurement of temperature, high theoretical limits of the measurable frequencies as well as high limits of the maximum strain and temperature. A fiber of the type SM 9/125μ-PI (INFAP GmbH) with three ingrained FBG in a single fiber with wavelengths of 1544 nm (strain), 1553 nm (strain) and 1564 nm (temperature) was used. The strain sensors were placed closer to the node while the temperature sensor was placed closer to the tool, as shown in Fig. 3. To avoid contact of the cable with the tool the fiber was placed lengthwise on the outside of the sonotrode with the cable being routed along the mount of the system. For this a canal

was milled where the fiber is placed inside of. A secure mount is enabled by afterwards filling the hole with an epoxy resin (EPO-TEK 353ND). All necessary alterations of the ultrasonic system were considered in the design process. For the measurements during free vibration a CLV-2534 compact laser vibrometer (Polytec GmbH) was used to measure the displacements at the front end of the sonotrode.

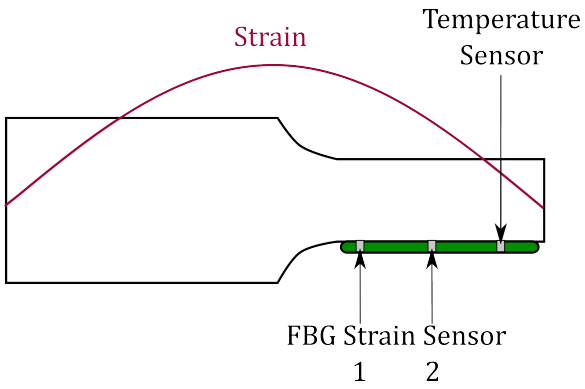


Fig. 3 Placement of the three fiber bragg gratings for measuring strain and temperature on the sonotrode

The position of the two fiber-optical sensors is given in Fig. 4. The design changes which were necessary for the incorporation of the sensors were also analyzed using the model. As the change in mass and geometry is negligible deviations are small.

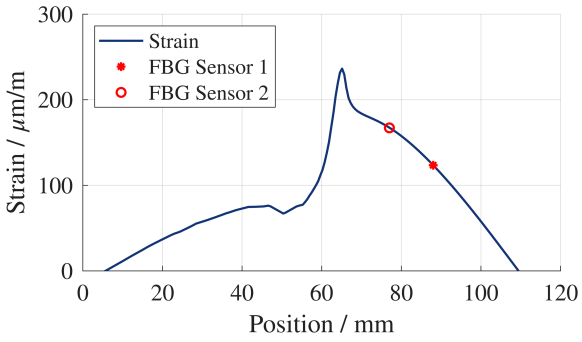


Fig. 4 Calculated strain along the length of the sonotrode and position of the two fiber optical strain sensors for $u = 100$ V.

2.3 Experimental setup

All sensors were applied to the ultrasonic system as described above. During the experiments the signals from the accelerometer, the passive piezoelectric disk, the voltage and the current from the ultrasonic generator as well as the signal from the 1D laser vibrometer, where applicable, were sampled at a frequency of 96,000 Hz using a Quantum MX410B (Hottinger Brüel and Kjaer) data acquisition system. The signals from the fiber optical sensors were processed using an interrogator (INFAP GmbH) to convert the light into electrical signals. The data for all three sensor elements (2x strain, 1x temperature) were sampled at 100,000 Hz. Prior to the machining experiments the system behavior as well as the data provided from the sensor systems was examined during free vibration to determine the resonance frequencies, the corresponding displacement near the tool as well as the measured strains, accelerations and temperature. Aside from the mechanical quantities, the supplied voltage and current during operation were also monitored. An impedance analysis was carried out first to determine the electrical resonance frequency of the ultrasonic system consisting of the transducer and sonotrode. The electrical resonance frequency for the longitudinal vibration is at $f_{res} = 22{,}845$ Hz. Then the system was excited with a frequency sweep ranging from 20,000 Hz to 25,000 Hz with a voltage of 10 V. The gathered data was also compared to a three dimensional, optical vibration measurement using a PSV-500 3D-laser-vibrometer (Polytec GmbH). The results from the preliminary experiments are shown in Fig. 5. The mechanical resonance frequency of the longitudinal mode can be seen at 22,850 Hz. Two additional peaks can be seen. The peak at 12,016 Hz correlates to a subharmonic of the longitudinal vibration, where only one node exists at the contact point of the transducer and sonotrode. A second mode was identified at 29,087 Hz, where the vibration is in a bending shape.

The chosen sensor systems were evaluated in a machining process to achieve a deeper understanding of their usability and the offered content of information during machining. As the kinematics of a turning process are relatively simple, there is no rotation of the tool and therefore an easy

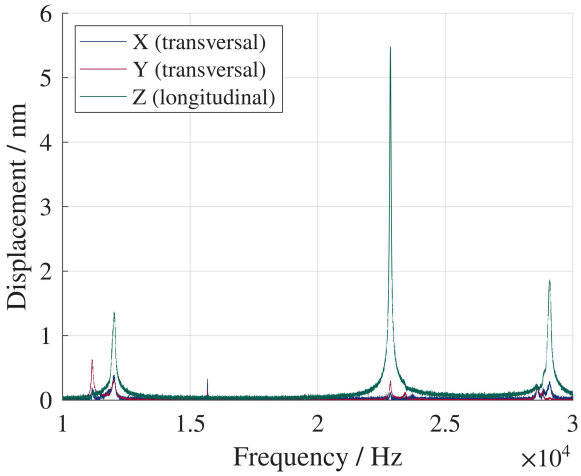


Fig. 5 Transfer function of the ultrasonic system for $u = 10$ V measured with the PSV-500 3D-laser-vibrometer

cable routing, an external cylindrical turning process was chosen for these experiments. For the workpiece material a bronze alloy (CuSn7Pb15-C) was chosen. The experiments were carried out on a PD 32 precision lathe (Spinner Werkzeugmaschinen GmbH). Prior to the ultrasonic vibration-superimposed turning process, the samples were premachined to a diameter of 30.2 mm. The experimental parameters are given in table 1. Aside from the machining parameters (cutting speed v_c, feed f, depth of cut a_p), the primary parameter of the ultrasonic system (power level) and with this the displacement x at the tool was varied. All parameters were examined three times for both variations of cutting speed and feed. For all parameter combinations one additional sample was machined without ultrasonic vibration superimposition as a reference sample for the sensor data and for the machined surface.

Table 1 experimental plan for the turning experiments

parameter	value / description
material	bronze (CuSn7Pb15-C)
sample dimension before pre-machining	d = 31 mm; l = 20 mm
tool	MCD tipped indexable insert CCGW 060202
clearance angle	25°
corner radius	0.09 mm
tool included angle	80°
cutting edge angle	50°
nominal rake angle	0°
depth of cut a_p	0.01 mm; 0.1 mm; 1 mm
operating frequency f	22,770 Hz
vibration direction	radially
cutting speed v_c	120 m/min; 480 m/min
feed f	0.05 mm; 0.1 mm
voltage u	38 V; 63 V; 98 V
displacement	2.4 μm; 5 μm; 6.5 μm
tool flank wear	0 μm; 50 μm; 100 μm

3 Results

3.1 Sensor data

3.1.1 Free vibration

The results for the strain data gathered with the two fiber optical sensors as well as the displacement at the tip of the sonotrode gathered with the 1D laser vibrometer are shown in Fig. 6 for different power levels. The system achieves maximum displacements at the tool of 6.5 μm at for a supplied voltage of 98 V. The maximum strain close to the node, where the highest strain occurs, is at 350 μm/m for FBG sensor 1. For FBG sensor 2 the strain is lower at 210 μm/m, which was expected from the strain curve in Fig. 4, but is higher than expected from the numerical simulations. Aside from low power levels where the signal-noise-ratio is considerably lower, the factor between FBG sensor 1 and FBG sensor 2 stayed constant at approximately 1.6. The displacement gathered from the 1D laser vibrometer and the calculated displacements based on the acceleration data match and are therefore not shown.

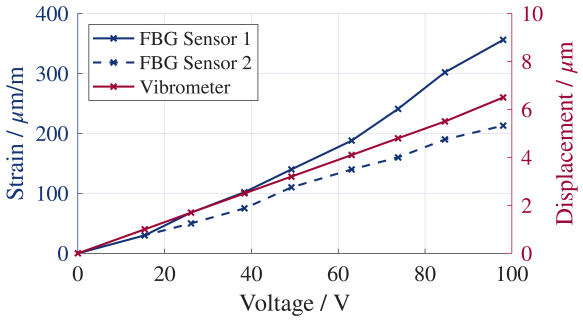


Fig. 6 Measured displacements and maximum strains at the sonotrode for different power levels

3.1.2 Accelerometer

For the analysis of the sensor signals the data from the turning experiment with $v_c = 120$ m/min, $f = 0.1$ mm and $u = 63$ V is shown in Fig. 7 for the acceleration data. The ultrasonic vibration started at 2.8 s (Fig. 7 a) and the generator ramped up the supplied voltage until vibration was stable starting from 4.4 s (Fig. 7 b). The ultrasonic vibration was stopped at 11.5 s (Fig. 7 e). For this experiment contact time between the tool was from 8.1 s until 10.4 s (Fig. 7 c-d). During operation of the ultrasonic system the measured acceleration amplitudes increased drastically to approximately 82,000 m/s^2 for a voltage of 63 V, which corresponds to a maximum displacement of 4.0 μm for the same voltage, which is the same as during free vibration. In the time domain the machining process is only slightly discernible as the process forces are too low to cause a decrease in the amplitudes. Instead a slight increase in accelerations can be seen in the time domain. This was caused by the generator which increased the supplied voltage during operation to keep the vibration constant.

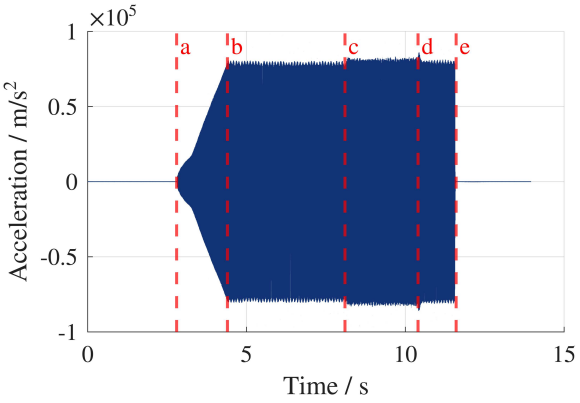


Fig. 7 Acceleration data during machining, $v_c = 120$ m/min, $f = 0.1$ mm, $u = 63$ V, a) start of the ultrasonic vibration b) start of stable vibration c) start of the turning process d) end of the turning process e) end of the ultrasonic vibration

3.1.3 Fiber optical sensor

Maximum strains are at 190 μm/m and 160 μm/m for FBG Sensor 1 and FBG Sensor 2, respectively, as seen in Fig. 8. In the beginning a slow increase of the measured strain is visible until the vibration is constant. The signal-noise-ratio is lower than that of the accelerometer. Additionally, a quantization error is apparent for low occurring strains. While the maximum positive strains are nearly the same, the compressive strains for FBG Sensor 1 are higher. Only a very low influence of the machining process can be seen in the time domain. When the tool gets in contact (from 8.1 s until 10.4 s) with the workpiece, the strains are reduced. One of the reasons is an additional damping caused by the machining process. Another reason might be a compression of the sonotrode caused by the process forces, as seen in [32]. As process forces are low the impact is low as well. The drop in the maximum achievable strain is compensated by an increase in the supplied voltage. This can be seen when the tool gets out of contact again at 10.4 s as the strain is higher and then drops off again, as seen in the accelerometer data.

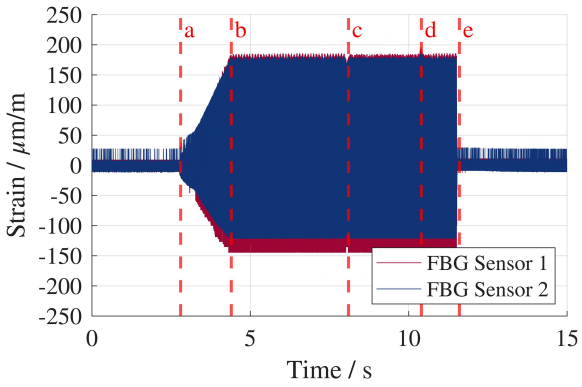


Fig. 8 Strain data during machining, $v_c = 120$ m/min, $f = 0.1$ mm, $u = 63$ V, a) start of the ultrasonic vibration b) start of stable vibration c) start of the turning process d) end of the turning process e) end of the ultrasonic vibration

For fiber-optical measurements of temperature the fibre is disconnected from the embedding so that a change in length is only caused by thermal expansion. Despite this, the ultrasonic vibration can still be seen in the time domain showing a sinusoidal temperature curve. A fourier transform confirms that the fiber vibrates at the operating frequency causing errors during the measurement. As an increase in temperature is still visible over time, a wandering mean value is used to

approximate the current temperature of the system during operation. From Fig. 9 it can be seen that the temperature stayed constant until the tool got in contact with the workpiece. After that the measured temperature increased, even after the machining process as well as the ultrasonic vibration was stopped. The temperature settled at 22 °C approximately 10 s after the vibration was stopped. After the experiment the temperature decreased again until the next machining process was started again. The quantization error as seen for the strain measurements is visible here as well. The highest temperature differences observable occurred during the experiments considering tool wear, where the maximum temperature difference was at 15 K.

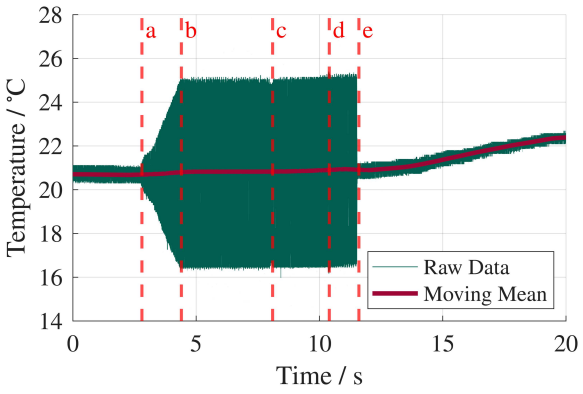


Fig. 9 Temperature data from the fiber optical sensor during machining, $v_c = 120$ m/min, $f = 0{,}1$ mm, $u = 63$ V, a) start of the ultrasonic vibration b) start of stable vibration c) start of the turning process d) end of the turning process e) end of the ultrasonic vibration

3.1.4 Passive piezoelectric disk

The measured voltage of the passive piezoelectric disk shows similar behavior as the other two sensor systems, shown in Fig. 10. During operation of the ultrasonic system a clear vibration can be seen in the time domain with an amplitude of 1.2 mV, but higher noise occurs for all measurements compared to the other sensors. For most experiments there was no discernible difference in the time domain for the machining process. As there no direct conversion of the measured voltages to displacement amplitudes at the tool is possible, the information gained from this sensor is low. After the vibration was stopped, peaks not resulting from the ultrasonic vibration can be seen at 12 s. These were caused when the carriage of the lathe stopped moving.

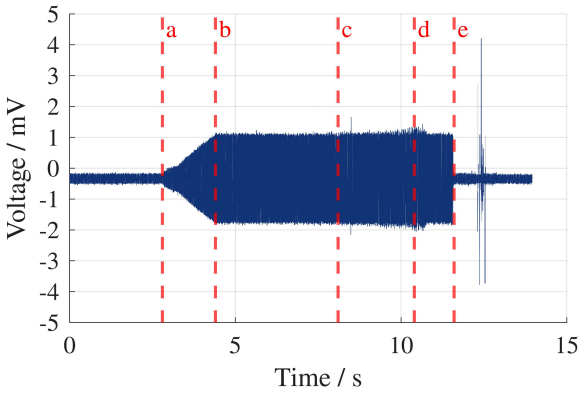


Fig. 10 voltage data from the passive piezoelectric disk during machining, $v_c = 120$ m/min, $f = 0.1$ mm, $u = 63$ V, a) start of the ultrasonic vibration b) start of stable vibration c) start of the turning process d) end of the turning process e) end of the ultrasonic vibration

3.2 Influence of cutting speed, feed and depth of cut

Cutting speed, feed and depth of cut show no discernible difference in the time domain of the sensor data. As the passive force acting axially on the sonotrode during the turning process should increase, an static offset of the strain should occur resulting from the compressive force acting on the sonotrode. As the largest force component occuring during machining is small (3.8 N for $a_p = 0.05$ mm and 8.2 N for $a_p = 0.1$ mm) the compression is also too small to affect the results. In the frequency domain the cutting speed is visible at 21 Hz and 84 Hz for cutting speeds of 120 m/min and 480 m/min, respectively, albeit with a significantly lower amplitude than the operating frequency of the ultrasonic system. The most prominent influence of the cutting speed and feed is the manufactured surface structure. The structure length is at approximately 330 μm for a cutting speed of 480 m/min as expected. The phase shift between two neighboring structures is also in line with the feed. However, the amplitude of the surface structure is at 11 μm for a measured vibration amplitude at the tip of the sonotrode of

4.8 μm. This behavior is also observable for different power levels of the ultrasonic system and therefore different measured vibration amplitudes at the tool. The factor between the expected and resulting amplitude is constant for all parameter combinations at 2.2 - 2.3 as seen in Fig. 14 and may indicate a systematic error of the whole setup.

3.3 Influence of tool flank wear

In Fig. 11 the influence of an increasing tool flank wear land width (100 μm) on the measured strains is shown. It can be seen that when the tool got in contact with the workpiece the maximum strains drop off, increasing with higher wear. The integrated control of the ultrasonic generator adjusted the power accordingly and the previous level of strain is achieved quickly. After the tool went of out contact with the workpiece, the strains increased inversely, as the power level was increased. The control system adjusted the power level as well and the maximum strain dropped off again. No effect of increasing tool flank wear on the acceleration data is visible. It stands to reason that higher wear, and therefore a higher contact width between the tool and workpiece causes higher forces acting on the system leading to a compressive strain.

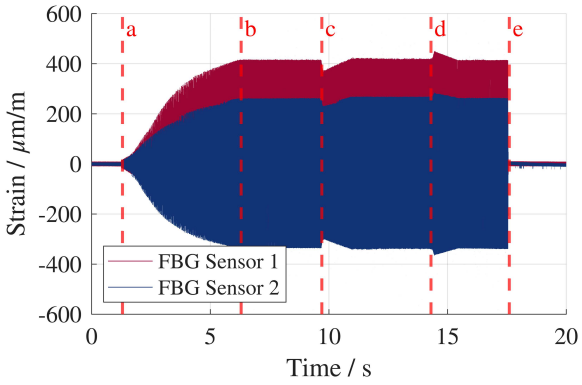


Fig. 11 Influence of tool flank wear on the measured strains, $v_c = 480$ m/min, $f = 0.1$ mm, $u = 98$ V, tool flank wear = 100 μm, a) start of the ultrasonic vibration b) start of stable vibration c) start of the turning process d) end of the turning process e) end of the ultrasonic vibration

4 Discussion

The sensors, especially the accelerometer and the fiber optical strain sensor seem useful for monitoring the in-process behavior. The predicted data from the numerical model, the data gathered during free vibration and during machining shows nearly identical behavior and the current operating frequency can easily be calculated. For low machining forces no dropoff in the vibration amplitude, either of the acceleration or strain, occured. For higher occurring forces and therefore a decrease in the available displacement at the tool is visible for the strain measurement, making a control possible. The most prominent discrepancy is the difference between the measured and calculated displacements close to the tool to the depth of the manufactured surface structure. Occurring process forces and a theoretical higher damping of the system during machining would suggest otherwise. To examine this deviation, several theories are proposed in each of the following sections.

4.1 Calculation errors

As the displacement occurring during the machining process is only calculated by the double integration of the acceleration data, a possible hypothesis for the deviations is an inaccurate calculation of the displacement based on this. To examine this the system was setup in a lab setting using the 1D laser vibrometer to measure the vibration at the tip of the sonotrode and to compare this result to the calculated displacements based on the acceleration data for different power levels. As seen in Fig. 12 the measured and calculated displacements are nearly identical, therefore an inaccurate calculation can be ruled out.

4.2 Influence of the additional tapering caused by the tool

As described previously, a tapering of the sonotrode is used to increase the displacement available at the tool. The increase in displacement is caused by a decrease of the cross-section of the ultrasonic system. As the tool for the machining process slightly protrudes over the front edge of the sonotrode and with this also over the measuring point of the accelerometer and the 1D laser vibrometer, a possible reason for the

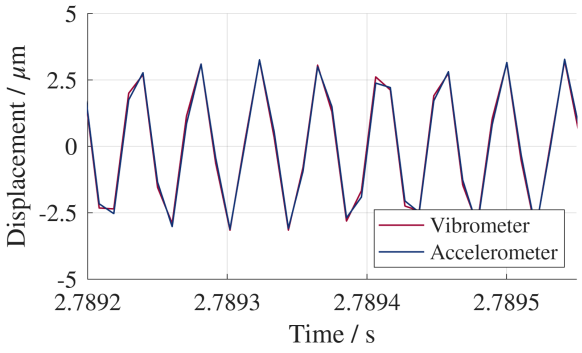


Fig. 12 Comparison of measured and calculated displacements for $u = 38$ V during free vibration

deviations could stem from an additional amplification caused by the unintended tapering caused by the tool. To examine this the calculated displacements are compared to the displacements measured directly at the cutting edge of the tool. As the tool has a pointed tip a direct measurement with a 1D laser vibrometer is not possible. Therefore the tip of the indexable insert was grinded off to achieve a flat surface to enable the measurement, as shown in Fig. 13. Then measurements during free vibration for different power levels (38 V, 63 V, 98 V) were carried out as well. Again, no differences between the calculated displacements at the tip of the sonotrode and the measured displacements at the cutting edge occurred. Therefore the additional tapering caused by the protrusion of the tool seems to have no effect on the deviations.

4.3 Influence of the machined material and geometry

As the displacements during free vibration are constant for different power levels, it stands to reason that the deviations were caused by the machining process itself. Firstly, the workpiece might have a resonance frequency close to the resonance frequency of the system causing an additional vibration in the process, which would not be measurable with the setup used. For this the geometry of the workpiece (d = 50 mm) and the material (EN AW 5083) were varied. To rule out a vibration of the workpiece in the workpiece mount two capacitive displacement sensors (capaNCDT 6200 CS02) were used and arranged 90° and 180° around the circumference of the workpiece relative to the tool. For machining the same parameters as described in Table 1 were used. For each parameter combination a workpiece was machined without ultrasonic vibration superimposition as a reference. The data from the previously used sensor system shows no difference to the previous experiments. The capacitive displacement sensors also show no vibration at either points observed. Despite this, the machined surface structure still shows an increased depth of the structure. The factor between the surface depth expected based on the calculated displacements and the measured surface depth is constant at 2.2 as seen in the previous experiments, see Fig. 14. Therefore the material and workpiece geometry seem to have no effect on the deviations.

4.4 Influence of external cylindrical turning

Another hypothesis for the deviations is that the kinematics of the external cylindrical turning process affect the outcome. Therefore experiments with the bronze workpiece were carried out in a face turning process. With this a higher stiffness of the machining process caused by the axial mounting of the workpiece was examined. As machining parameters the cutting speed and feed were varied while the depth of cut was kept constant at 0.1 mm. As the workpieces are tubular with an outer diameter of 31 mm and an inner diameter of 20 mm only a width of 5.5 mm were machined. Only a single power level (63 V) was considered for the experiments. For each parameter combination a workpiece was machined without ultrasonic vibration superimposition as a reference. The sensor data for the accelerometer and the fiber optical sensors shows the same behavior as previously described. Only the passive piezoelectric disk shows an increase of the measured voltage amplitudes during machining. In the frequency domain it can be seen that this behavior can be attributed to the increasing rotational speed of the spindle as the same behavior occurs for the experiments without ultrasonic vibration superimposition. The sinusoidal shaped surface structure had an amplitude of 10.1 μm while the calculated displacement at the tool was at 4.2 μm, showing deviations with a factor of 2.4.

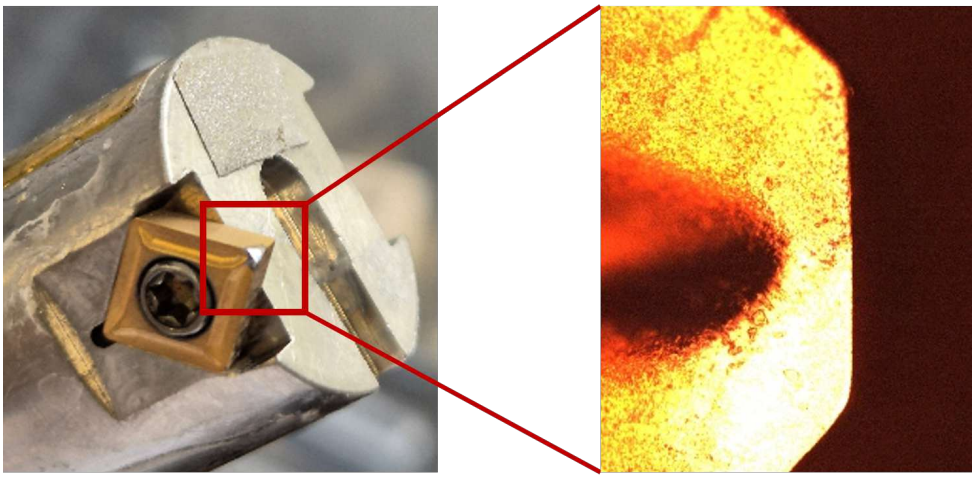


Fig. 13 Tool with the grinded insert for the comparisons of the measured and calculated displacements

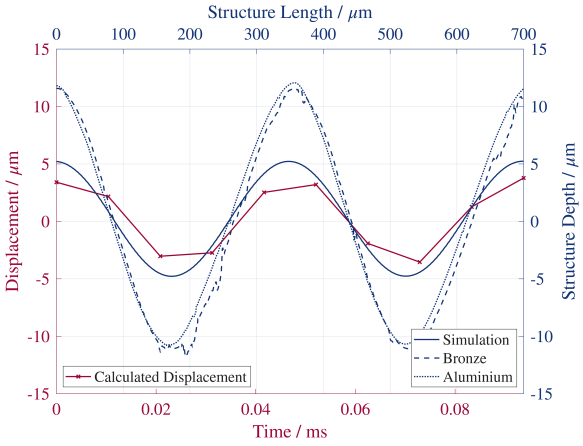


Fig. 14 Machined and expected surface structure (blue) of an aluminium workpiece as well as calculated displacement (red) during vibration for $v_c = 480$ m/min, $f = 0.1$ mm, $u = 63$ V

5 Conclusion

This study presents an approach for measuring ultrasonic vibrations in an external cylindrical turning process to monitor the occurring accelerations and strain, enable an in-process-prediction of the achievable displacement at the tool and predict the manufactured surface structure. The accelerometer has the main advantage of enabling a direct calculation of the displacement close to the tool by double integration. The experiments show a high congruence of the calculated displacement and a reference measurement using a 1D laser vibrometer. Beside the displacement, shifts in the resonance frequency could also be detected using an accelerometer. As there are no direct limitations regarding the sampling rates of the acceleration data, the accelerometer is suited well for the frequency and displacement control in ultrasonic systems. The biggest disadvantage is that static or quasi-static components can not be detected well. The fiber-optical strain measurements are more advantageous in that regard as they can detect a static compression more easily. Their suitability for a use in a control system is limited by their technical boundaries. First, the light has to be converted into an electrical signal which affects the real-time applications. Secondly, the maximum sampling rates are 100,000 Hz, which only yields approximately four sampling points per period of the vibration. This might not prove high enough for control systems where a high resolution of the sinusoidal wave is necessary. The temperature measurement provides an additional amount of information of the system behavior, but can easily be substituted with different measurement solutions. As no substantial build-up of heat was observed, the information gain is limited.

While the length of the structure and the shift between neighboring structures can be predicted with high accuracy based on the ultrasonic parameters (operating frequency) in combination with the machining parameters (cutting speed, feed), the depth of the surface structure can not be predicted accurately as there is a deviation between the predicted and the actual depth of the structure. Several possible causes for this are discussed

and examined experimentally. With this, calculation errors, the influence of the protruding tool, different workpiece materials and geometries as well as the influence of the process kinematics are ruled out as the deviations are constant for all causes considered.

Depending on the sensor system used, specific information can be gathered from the sensor signals. First vibrations from the machining process itself can be distinguished from the ultrasonic vibration. Furthermore, an increase of forces acting axially on the system, in this work caused by an artificially generated flank tool wear shows a decrease in measured strain, which was not visible in the data from the passive piezoelectric disk at the transducer, indicating a better suitability of the strain measurement for a more precise control of the vibration amplitude during operation. However it is still uncertain how this changes for harder to machine materials and therefore higher process forces. Finally the reasons and mechanisms for the increase in structure depth compared to the expected depth are still unknown. For this the influence of sonotrode and tool geometry needs to be examined. However, a change in either the sonotrode or the tool geometry, which comes with modifications of the sonotrode as well, would affect the resonance frequency of the system and might therefore invalidate the results. Nonetheless, the influence of sonotrode and tool geometry will be examined in a future work.

Declarations

Funding

This research was funded by the Deutsche Forschungsgemeinschaft (DFG, German Research Foundation) - grant number 510749881.

Competing Interests

The authors have no relevant financial or non-financial interests to disclose.

CRediT Author Contributions

Jonas Maximilian Werner: Conceptualization, Methodology, Formal analysis, Investigation, Writing - Original Draft, Visualization. **Hendrik Liborius:** Conceptualization, Methodology, Formal analysis, Investigation. **Andreas Schubert:** Conceptualization, Writing - Review & Editing, Supervision, Project administration, Funding acquisition. **Welf-Guntram Drossel:** Conceptualization, Writing - Review & Editing, Supervision, Project administration, Funding acquisition.

Data availability

Data will be made available upon request.

Ethics approval and consent to participate

Not applicable.

Materials availability

Not applicable.

Code availability

Not applicable.

References

[1] G. Shao, H. Li, M. Zhan, A Review on Ultrasonic-Assisted Forming: Mechanism, Model, and Process, Chines Journal of Mechanical Engineering 34 (2021) 1-24.

[2] H. Li, J. Liu, C. Shen, C. Li, An Ultrasonic Vibration-Assisted Superplastic Forming Method for Zr-Based Bulk Amorphous Alloys: Experiment and Simulation, Metals 15(12) (2025) 1299.

[3] X.M. Cheng, K. Yang, J. Wang, W.T. Xiao, S.S. Huang, Ultrasonic system and ultrasonic metal welding performance: A status review, Journal of Manufacturing Processes 84 (2022) 1196-1216.

[4] C. Zhang, J. Zhang, P. Feng, Mathematical model for cutting force in rotary ultrasonic face milling of brittle materials, The International Journal of Advanced Manufacturing Technology 69 (2013) 161-170.

[5] S.S.F. Chang, G.M. Bone, Burr size reduction in drilling by ultrasonic assistance, Robotics and Computer-Integrated Manufacturing 21 (2005) 442-450.

[6] R. Singh, J.S. Khamba, Mathematical modeling of tool wear rate in ultrasonic machining of titanium, The International Journal of Advanced Manufacturing Technology 43 (2009) 573-580.

[7] F. Feucht, J. Ketelaer, A. Wollf, M. Mori, M. Fujishima, Latest Machining Technologies of Hard-to-cut Materials by Ultrasonic Machine Tool, Procedia CIRP 14 (2014) 148-152.

[8] N.F.H.A. Halim, H. Ascroft, S. Barnes, Analysis of Tool Wear, Cutting Force, Surface Roughness and Machining Temperature During Finishing Operation of Ultrasonic Assisted Milling (UAM) of Carbon Fibre Reinforced Plastics (CFRP), Procedia Engineering 184 (2017) 185-191.

[9] M. Khajehzadeh, O. Boostanipour, M.R. Razfar, Finite element simulation and experimental investigation of residual stresses in ultrasonic assisted turning, Ultrasonics 108 (2020) 106208.

[10] P. Du, W. Chen, J. Deng, S. Zhang, J. Zhang, Y. Liu, A critical review of piezoelectric ultrasonic transducers for ultrasonic-assisted precision machining, Ultrasonics 135 (2023) 107145.

[11] S. Yin, W.S. Yip, Z. Dong, R. Kang, S. To, Theoretical and experimental investigations on phase difference in ultrasonic elliptical vibration cutting of tungsten alloys, Ultrasonics 156 (2025) 107773.

[12] H. Martins, H. Puga, Ultrasonic Assisted Machining Overview: Accessing Feasibility and Overcoming Challenges for Milling Applications, Metals 13(5) (2023) 908.

[13] W.X. Xu, L.C. Zhang, Ultrasonic vibration-assisted machining: principle, design and application, Advances in Manufacturing 3 (2015) 173-192.

[14] J.A. Gallego-Juarez, K.F. Graff, Power Ultrasonics Applications of high-intensity ultrasound, Amsterdam: Woodhead publishing (2015).

[15] C. Yang, X. Shan, T. Xie, Titanium wire drawing with longitudinal-torsional composite ultrasonic vibration, The International Journal of Advanced Manufacturing Technology 83 (2016) 645-655.

[16] S. Amini, M.R. Khosrojerdi, R. Nosouhi, Elliptical ultrasonic-assisted turning tool with longitudinal and bending vibration mode, Proceedings of the Institution of Mechanical Engineers, Part B: Journal of Engineering Manufacture 231 (2017) 1389-1395.

[17] M. Nad, Ultrasonic horn design for ultrasonic machining technologies, Applied and Computational Mechanics 4 (2015) 79-88.

[18] E. Shamoto, N. Suzuki, T. Moriwaki, Y. Naoi, Development of Ultrasonic Elliptical Vibration Controller for Elliptical Vibration Cutting, CIRP Annals 51 (2002) 327-330.

[19] R. Zhang, P. Steinert, A. Schubert, Microstructuring of Surface by Two-stage vibration assisted Turning, Procedia CIRP 14 (2014) 136-141.

[20] A. Schubert, A. Nestler, S. Pinternagel, H. Zeidler, Influence of ultrasonic vibration assistance on the surface integrity in turning of the aluminium alloy AA2017, Materialwissenschaft und Werkstofftechnik 42 (2011) 658-665.

[21] A. Nestler, A. Schubert, Surface Properties in Ultrasonic Vibration Assisted Turning of Particle Reinforced Aluminium Matrix Composites, Procedia CIRP 12 (2014) 125-130.

[22] S. Xu, T. Kuriyagawa, K. Shimada, M. Mizutani, Recent advances in ultrasonic-assisted machining for the fabrication of micro/nano-textured surfaces, Frontiers of Mechanical Engineering 12 (2017) 33-45.

[23] S. Wei, P. Zou, L. Fang, J. Duan, Microstructure evolution of medium carbon steel during heat-assisted 3D ultrasonic vibration-assisted turning, Ultrasonics 135 (2023) 107129.

[24] Z. Peng, X. Zhang, D. Zhang, Effect of radial high-speed ultrasonic vibration cutting on machining performance during finish turning of hardened steel, Ultrasonics 111 (2021) 106340.

[25] H. Zhou, S.H. Huang, W. Li, Electrical Impedance Matching between Piezoelectric Transducer and Power Amplifier, IEEE Sensor Journal 20 (2020) 14273-14281.

[26] H. Yokozawa, J. Twiefel, M. Weinstein, T. Morita, Dynamic resonant frequency control of ultrasonic transducer for stabilizing resonant state in wide frequency band, Japanese Journal of Applied Physics 56 (2017) 07JE08.

[27] S. Voronina, V. Babitsky, Autoresonant control strategies of loaded ultrasonic transducer for machining applications, Journal of Sound and VIbration 313 (2008) 395-417.

[28] X. Li, A. Meadows, V. Babitsky, R. Parkin, Experimental analysis on autoresonant control of ultrasonically assisted drilling, Mechatronics 29 (2015) 57-66.

[29] J.M. Werner, M. Engelmann, M. Schmidt, C. Titsch, M. Dix, W.-G. Drossel, Comparison of Structural Integrated Piezoceramics, Piezoelectric Patches and Strain Gauges for Condition Monitoring 22 (2022) 1-15.

[30] X. Li, V. Babitsky, R. Parkin, A. Meadows, Autoresonant excitation and control of nonlinear mode for ultrasonically assisted drilling, ZAMM Journal of Applied Mathematics and Mechanics 94 (2014) 904-910.

[31] J.M. Werner, M. Hansen, W.-G. Drossel, Influence of External Forces on the Detectability of the Resonance Frequency of Ultrasonic Vibration Systems, Production at the Leading Edge of Technology (2025) 65-72.

[32] S. Kimme, N. Hafez, C. Titsch, J.M. Werner, A. Nestler, W.-G. Drossel, Close-to-process strain measurement in ultrasonic vibration-assisted turning, Journal of Sensors and Sensor Systems 8 (2019) 285-292.

[33] J.M. Werner, H. Liborius, W.-G. Drossel, A. Schubert, In-process measurement of vibrations in ultrasonic vibration superimposed turning using mechanical feedback signals, Procedia CIRP 138 (2026) 409-414.

[34] J.M. Werner, T. Krüger, W.-G. Drossel, Feasibility Study for Monitoring an Ultrasonic System Using Structurally Integrated Piezoceramics, Sensors 24(3) (2024) 1036.

[35] Ceramtec, Datasheet Piezo Hard Materials, online: https://www.ceramtec-industrial.com/fileadmin/user_upload/Corporate/11_Downloads/04_Piezo_Ceramics/CeramTec_Datasheet_Piezo_Hard_Materials_EN.PDF (2026).

[36] M. Mirzabagherian, S. Amini, M. Bayat, Investigation of the effects of ultrasonic assisted face turning with CO2 cooling on cutting forces, residual stress, and surface quality, International Journal of Lightweight Materials and Manufacture 8 (2025) 551-561.

[37] A.T. Bui, T.V.C. Tran, K.H. Nguyen, H.P. Nguyen, D.K. Bui, The Future of Ultrasonic-Assisted Turning: Development Directions and Research Prospects, EAI International Conference on Renewable Energy and Sustainable Manufacturing (2024) 281-296.

[38] T.-T. Nguyen, T.-T. Vu, T.-D. Nguyen, Surface Topography in Cutting-Speed-Direction Ultrasonic-Assisted Turning, Micromachines 15(6) (2024) 668.

[39] J.M. Werner, M. Gerber, W.-G. Drossel, Model-based Approach for a Control System for Ultrasonic Systems Using Mechanical Sensors, Production at the Leading Edge of Technology (2026) 210-219.